New Phytologist

Cyclophilin A-mediated *cis/trans* isomerization modulates RIN4 to control intracellular rhizobial infection in legumes

Takashi Goto[1,2], Kasper Røjkjær Andersen[1], Masaru Bamba[3,4], Shusei Sato[3], Masayuki Sugawara[5], Kiwamu Minamisawa[3], Masayoshi Kawaguchi[2,6], Jens Stougaard[1] and Yasuyuki Kawaharada[7]

[1]Department of Molecular Biology and Genetics, Aarhus University, Universitetsbyen 81, Aarhus C, 8000, Denmark; [2]National Institute for Basic Biology, 38 Nishigo-naka, Myodaiji, Okazaki, Aichi, 444-8585, Japan; [3]Graduate School of Life Sciences, Tohoku University, 2-1-1 Katahira, Aoba-ku, Sendai, Miyagi, 980-8577, Japan; [4]Faculty of Agriculture, Shizuoka University, 63 Kariyado, Fujieda, Shizuoka, 426-0001, Japan; [5]Department of Life and Food Sciences, Obihiro University of Agriculture and Veterinary Medicine, West 2-11, Inada, Obihiro, Hokkaido, 080-8555, Japan; [6]School of Life Science, The Graduate University for Advanced Studies (SOKENDAI), Okazaki, Aichi, 444-8585, Japan; [7]Department of Biosciences, Faculty of Agriculture, Iwate University, 3-18-8 Ueda, Morioka, Iwate, 020-8550, Japan

Authors for correspondence:
Takashi Goto
Email: tgoto@mbg.au.dk

Yasuyuki Kawaharada
Email: yasuyuki@iwate-u.ac.jp

Received: *9 January 2026*
Accepted: *13 March 2026*

New Phytologist (2026) **250:** 3932–3945
doi: 10.1111/nph.71147

Key words: *cis/trans* isomerization, Cyclophilin A, immune system modulation, *Lotus japonicus*, *Mesorhizobium loti*, RIN4, root nodule symbiosis, type III secretion system.

Summary

- In most legume-rhizobium symbioses, rhizobial colonization occurs through host-derived intracellular infection threads, which enable rhizobial recruitment while presumably modulating the host immune system to prevent rejection. To investigate post-*trans*lational regulation of immune responses during rhizobial infection, we focused on Cyclophilin A (CyPA), a peptidyl-prolyl *cis/trans* isomerase.
- The model legume *Lotus japonicus* encodes three canonical *CyPA* genes. Using CRISPR/Cas9 mutagenesis, structural modeling, and phylogenomics, we characterized *LjCyPA1* as essential for normal intracellular infection by compatible rhizobia. A gain-of-function *LjCyPA1* variant in a soybean cultivar promoted symbiosis with both compatible and incompatible rhizobia.
- Functional association between LjCyPA1 and the immune hub protein LjRIN4 is essential for symbiosis. The putative *cis*-LjRIN4 promoted intracellular rhizobial infection, while the putative *trans*-LjRIN4 suppressed it. LjCyPA1 and LjRIN4 acted in concert with the rhizobial type III secretion system (T3SS), highlighting a cooperative role between host and symbiont in facilitating infection.
- Our results contribute to the understanding of how legumes accept symbiotic partners while balancing immune responses.

Introduction

A fundamental question in symbioses research centers on how plant hosts engage with symbionts. Legume plants interact with nitrogen-fixing bacteria called rhizobia, selectively hosting those that meet specific criteria as beneficial endosymbionts. The legume–rhizobia symbiosis, widely known as root nodule symbiosis, serves as a model system for understanding the host's decision-making in accepting compatible symbionts. Legumes perceive rhizobial lipochitooligosaccharides (Nod factors) via the cell-surface receptors NFR1/LYK3 and NFR5/NFP (Limpens *et al.*, 2003; Madsen *et al.*, 2003; Radutoiu *et al.*, 2003; Smit *et al.*, 2007; Indrasumunar *et al.*, 2010, 2011; Broghammer *et al.*, 2012). The authentication of rhizobia is further ensured by recognition of bacterial exopolysaccharide (EPS) by the EPR3 receptor (Kawaharada *et al.*, 2015, 2017b; Kelly *et al.*, 2023). The structure and modifications of Nod factor and EPS are bacteria specific and enable legume–bacteria pairing (López-Lara *et al.*, 1996; Roche *et al.*, 1996; Skorupska *et al.*, 2006; Radutoiu *et al.*, 2007; Kawaharada *et al.*, 2015). Upon recognizing compatible signals, legumes initiate a symbiotic signaling pathway leading to rhizobial infection and nodule formation. Two different modes of infection routes are found in legumes: intracellular and intercellular infection. The intracellular route observed in *c.* 75% of legume hosts transports rhizobia from epidermal root-hair cells into cortical cells via tunnel-like tubular structures called infection threads (ITs). In the intercellular route, rhizobia invade through cracks between epidermal cells formed during lateral root emergence (Quilbé *et al.*, 2022). Intracellular infection is more efficient than intercellular infection since the host actively invites rhizobia, contingent upon those rhizobial molecules meeting stricter criteria (Madsen *et al.*, 2010; Kawaharada *et al.*, 2017b; Acosta-Jurado *et al.*, 2019; Montiel *et al.*, 2021).

Successful symbiosis requires not only these infection modes but also proper regulation of the immune response that would otherwise reject symbionts. Nod factor perception induces phosphorylation of downstream factors and suppresses the production

of reactive oxygen species (ROS; Shaw & Long, 2003; Liang *et al.*, 2013; Rey *et al.*, 2019; Feng *et al.*, 2021; Wang *et al.*, 2025). Cytoplasmic kinases LICK1/2 simultaneously activate symbiotic signaling via *trans*-phosphorylation of LYK3 and suppress the immune response (Wang *et al.*, 2025). These insights highlight the importance of immune suppression for successful symbiosis, yet much is still unknown on how the immune system is modulated during rhizobial infection. Plant immunity consists of two immune systems: microbe/pathogen-associated molecular patterns (MAMPs/PAMPs)-triggered immunity (MTI/PTI) and effector-triggered immunity (ETI). MTI/PTI is a basal immune response triggered by common microbial patterns. To suppress this defense, bacteria deliver effector proteins into host cells, but host plants carrying the corresponding resistance (R) genes recognize these effectors and counterattack with ETI (Jones & Dangl, 2006). Interestingly, rhizobia also attempt to promote infection through effectors known as nodulation outer proteins (Nops) (Marie *et al.*, 2001; Cao *et al.*, 2017; Miwa & Okazaki, 2017; Piromyou *et al.*, 2021; Ma *et al.*, 2024), suggesting that these effectors promote symbiosis in the context of compatible interactions. By contrast, when certain rhizobia produce incompatible Nops, the host legume recognizes them and ETI blocks nodulation (Yang *et al.*, 2010; Tang *et al.*, 2016; Sugawara *et al.*, 2018; Zhang *et al.*, 2021). Unlike pathogenic interactions, where broad immune responses are typically effective against invaders, symbiosis requires the host legumes to properly modulate immunity depending on whether rhizobia are compatible or incompatible. This balance and immune flexibility support the robustness of the symbiosis system, which serves as a foundation for the host's environmental adaptability. However, the regulatory factors that enable this immune modulation in the intracellular infection system of legumes remain largely unexplored.

Cyclophilin (CyP) is a peptidyl-prolyl *cis/trans* isomerase that catalyzes the isomerization of proline residues between *cis* and *trans* conformation in target proteins. Among them, Cyclophilin A (CyPA) was first discovered in association with immunity in animal cells (Handschumacher *et al.*, 1984). In *Arabidopsis thaliana*, one of the CyPAs (AtCYP18-3, also known as AtROC1), interacts with RIN4 (Li *et al.*, 2014), the immune signaling hub involved in both MTI/PTI and ETI (Mackey *et al.*, 2002, 2003; Axtell & Staskawicz, 2003; Toruño *et al.*, 2018; Ray *et al.*, 2019). Intriguingly, AtCYP18-3/AtROC1, particularly its gain-of-function variant, reduces immune response to *Pseudomonas syringae* by suppressing ETI in leaves (Ma *et al.*, 2013; Li *et al.*, 2014), a function that may be counterproductive for the host. Here, we hypothesize that native CyPAs fulfill a beneficial function in symbiotic interactions. We analyzed homologous CyPAs in the context of root nodule symbiosis using the model legume *Lotus japonicus* and found that LjCyPA1 is required for normal intracellular infection of compatible rhizobia. The gain-of-function *LjCyPA1* variant exhibited enhanced symbiosis with both compatible and incompatible rhizobia. Structural modeling followed by genetic analysis suggested that *cis/trans* isomerization of LjRIN4 influences rhizobial acceptance during intracellular infection, which requires rhizobial effectors. LjCyPA1 is co-conserved with intracellular infection in legumes, and we discuss how the *cis/trans* isomerization of LjRIN4 contributes to acceptance of symbiotic partners during intracellular infection.

Materials and Methods

Plant materials and growth conditions

The *Lotus japonicus* Miyakojima MG-20 ecotype was used as wild-type (WT). The soybean cultivar used in this study was Hardee. Three-day-old MG-20 seedlings were transferred to culture vessels containing sterilized vermiculite with B&D medium and grown for 3 d to adapt. For bacterial growth, *Mesorhizobium loti* MAFF303099 (for *L. japonicus* symbiont) was cultured in Yeast Extract-Mannitol medium, while *Bradyrhizobium diazoefficiens* USDA122 (for soybean symbiont) was cultured in HEPES-MES (HM) salt medium (Cole & Elkan, 1973; supplemented with 0.1% arabinose and 0.025% (wt/vol) of yeast extract). For inoculation, rhizobia were suspended in B&D medium: *M. loti* MAFF303099 in Stock A-D (×1), pH 5.7; and USDA122 in Stock B (×0.5) and Stock C-D (×1) at pH 6.8. DsRed-labeled *M. loti* MAFF303099 was used for microscopic observation.

CRISPR/Cas9 mutagenesis

To generate *cypA1*, *cypA2*, and *cypA3* knockout plants using a CRISPR/Cas9 system, double-strand DNA oligos were designed using the CRISPR-P program (http://crispr.hzau.edu.cn/CRISPR2/) (Lei *et al.*, 2014). These oligos were cloned into the entry vector pUC_AtU6-oligo (Ito *et al.*, 2015). For gRNA expression, an I-SceI-digested gRNA module was inserted into the binary vector pZK _gYSA _FFCas9 (Ito *et al.*, 2015). For whole-plant transformation, *Agrobacterium tumefaciens* AGL1 strains were used. Hypocotyl segments from MG-20 WT were incubated on papers soaked in co-culture medium (1/10 Gamborg's B5 salt mixture, 1/10 Gamborg's vitamin solution, 0.5 μg ml^{-1} BAP, 0.05 μg ml^{-1} NAA, 5 mM MES (pH 5.2), and 20 μg ml^{-1} acetosyringone, pH 5.5) containing an AGL1 suspension for 5 d at 24°C in the dark. Next, the segments were transferred onto a callus induction medium (1× Gamborg's B5 salt mixture, 1× Gamborg's vitamin solution, 2% sucrose, 0.2 μg ml^{-1} BAP, 0.05 μg ml^{-1} NAA, 10 mM $(NH_4)_2SO_4$, 0.3% phytagel, 12.5 μg ml^{-1} meropen, and 15 μg ml^{-1} Hygromycin B, pH 5.5). They were cultured under a 16 h : 8 h, light : dark cycle at 24°C and transferred every 5 d for 2–5 wk. Once the calli turned deep green, they were transferred onto a shoot elongation medium (Gamborg's B5 salt mixture, Gamborg's vitamin solution, 2% sucrose, 0.2 μg ml^{-1} BAP, 12.5 μg ml^{-1} meropenem, 0.6% agar, pH 5.5) and grown for 3–6 wk under the same conditions. The calli were transferred onto a fresh callus induction medium every 7 d. The individual shoots from calli were excised and inserted into a root induction medium (1/2 Gamborg's B5 salt mixture, 1/2 Gamborg's vitamin solution, 1% sucrose, 0.5 μg ml^{-1} NAA, 0.9% agar, pH 5.5) and cultivated for 1–2 wk under the same conditions. Once root formation was evident, they were transplanted into root elongation medium (1/2 Gamborg's B5 salt mixture,

1/2 Gamborg's vitamin solution, 1% sucrose, and 0.9% agar, pH 5.5) for 2 wk under the same conditions.

Construction of ΔT3SS rhizobia

The type III secretion system (T3SS) mutant was constructed using a transconjugation system. Two genomic regions (*c.* 1 kb each) of *M. loti* MAFF303099 and the gentamicin cassette region from pMS246 (Becker *et al.*, 1995) were amplified by PCR, and cloned to pK18mob digested by *BamH*I using In-Fusion (Takara Bio Inc., Shiga, Japan) reaction. This plasmid was transformed into *M. loti* MAFF303099 harboring DsRed via triparental mating with *E. coli* strain MT616 carrying the mobilizing plasmid pRK600 (Finan *et al.*, 1986). Subsequently, a double-crossover mutant was selected based on gentamicin resistance and kanamycin sensitivity. The disrupted gene names are listed in Supporting Information Table S1 (Okazaki *et al.*, 2010).

Hairy root transformation

Hairy root transformation was carried out using *Agrobacterium rhizogenes* AR1193 (for *L. japonicus*) and K599 (for soybean). MG-20 and *cypA1* seedlings, grown for 3 d in darkness followed by 1 d under a 16 h : 8 h, light : dark cycle at 24°C, were excised below the hypocotyls while submerged in an AR1193 suspension containing the appropriate vectors. The seedlings were then co-cultivated on half-strength B5 medium (Wako, Osaka, Japan, or Duchefa Biochemie, Haarlem, the Netherlands) supplemented with 0.02 g l^{-1} sucrose, 0.5 g l^{-1} MES, and 0.9% agar at 24°C in darkness for 3 d. Subsequently, they were transferred to a hairy root induction medium (B5 medium with 1% sucrose, Gamborg B5 vitamin solution, 0.5 g l^{-1} MES, 12.5 μg ml^{-1} meropenem (Sumitomo Pharmaceuticals or Sigma-Aldrich), and 0.9% agar) and incubated for 10 d under a 16 h : 8 h, light : dark cycle at 24°C. Transgenic hairy roots were confirmed by green fluorescent protein (GFP) signal. Plants were inoculated with rhizobia 10 d after being transferred to vermiculite. The soybean cultivar Hardee seedlings were grown in culture vessels containing sterilized vermiculite for 5–7 d in darkness and then excised below the hypocotyls. The cut surfaces were coated with K599, and hairy roots were induced in the culture vessels. After 2 wk, non-GFP roots were removed, and plants were transplanted into the culture vessels and inoculated with rhizobia 10 d later.

RNA sequencing

Roots of MG-20 and the *cypA1* mutant, either without (0 d after inoculation (DAI)) or with 3 DAI of the *M. loti* ΔT3SS mutant, were harvested. Total RNA was isolated using the RNeasy Plant Mini Kit (Qiagen, Hilden, Germany), and DNA was removed by DNase treatment (Qiagen). Libraries were sequenced using an MGI DNBSEQ-T7, generating paired-end reads. All reads were quality-checked by FastQC and adapter trimmed with Trimmomatic (v.0.33, options: LEADING : 20 TRAILING : 20 SLIDINGWINDOW : 4 : 15 MINLEN : 30). Reads were then mapped to the genome (Gifu v.1.2 model) using Hisat2 (v.2.1.0). Read counts were obtained using HTSeq (v.2.0.7). Normalization and extraction of differentially expressed genes (DEGs) were performed on iDEGES/edgeR–edgeR pipeline in the TCC R package.

Gene expression analysis

Primers used for quantitative reverse transcription polymerase chain reaction (qRT-PCR) are listed in Table S2. Total RNA was isolated from roots using NucleoSpin RNA Plant (Macherey-Nagel, Düren, Germany). First-strand cDNA was prepared using Maxima H Minus First Strand cDNA Synthesis Kit (Thermo Fisher Scientific, Tokyo, Japan). qRT-PCR was performed with LyghtCycler 480 SYBER Green I Master (Roche) on CFX96 Real Time System (Bio-Rad) following the manufacturer's instructions. Expression of *LjUBQ* was used as a reference.

Phylogenetic and phylogenomic analysis

Protein and genome sequences obtained from the NCBI Genome database and Phytozome v.12 (https://phytozome.jgi.doe.gov/pz/portal.html) were used. Alignment of sequences was performed using Clustal X. To analyze synthetic relationships between *L. japonicus* and multiple plant species, we used the JCVI toolkit (https://github.com/tanghaibao/jcvi). Orthologous gene pairs were identified using the jcvi.compara.catalog ortholog command with protein-coding sequences across 17 species: *Medicago truncatula*, *Trifolium pratense*, *Cicer arietinum*, *Glycine max*, *Glycine soja*, *Vigna angularis*, *Vigna radiata*, *Abrus precatorius*, *Arachis ipaensis*, *Arachis duranensis*, *Lupinus albus*, *Lupinus angustifolius*, *Aeschynomene evenia*, *Fragaria vesca*, *Malus domestica*, *Populus trichocarpa*, and *Arabidopsis thaliana*. Syntenic blocks were detected using MCScan (Wang *et al.*, 2012) implemented in JCVI, by comparing *L. japonicus* gene coordinates against synteny anchors, iterating 20 times to refine predictions. For visualization, we followed the JCVI manual guidelines. In the graphical representation, due to polyploidy, only one chromosome was used for *Glycine max*, *Glycine soja*, and *Malus domestica* (e.g. *CyPA1*-associated synteny was observed on Chromosomes 4 and 6 of *G. max* and *G. soja*, and on Chromosomes 5 and 10 of *Malus domestica*).

Site-directed mutagenesis of CyPA1 and RIN4

The coding sequences of *LjCyPA1* and *LjRIN4* were amplified from *L. japonicus* MG-20 cDNA. Each PCR fragment was cloned into pENTR/D-TOPO (Invitrogen). *LjCyPA1* variants (gain-of-function: S58F; binding defective: F67A; catalytic defective: H133A) and *LjRIN4* variants (*cis*-conformation mimic: ΔP187, *trans*-conformation mimic: P187V) were generated using the PrimeSTAR Mutagenesis Basal Kit (Takara). The primers are listed in Table S2. Along with the original *LjCyPA* and *LjRIN4*, their respective variants in pENTR/D-TOPO were recombined into the modified Gateway binary vector, proLjUBQ:GW-GFP.

Protein modeling

AlphaFold2 was used to generate the models of LjCyPA1 and AtCYP18-3/ROC1. No template was used in the modeling

process. Structural analysis and figures were made in PyMOL v.3.1.1 (Schrödinger, LLC).

Microscopy

Fluorescence microscopy was performed using a BX50 upright microscope (Olympus, Tokyo, Japan) and confocal microscopes (Nikon A1R; Zeiss LSM780, Tokyo, Japan). Images were acquired and analyzed using DP Controller (Olympus), NIS Elements (Nikon), and ZEN software (Zeiss). Following excitation/emission (nm) settings were used: autofluorescence of cell components, 405/420–505; DsRed, 561/580–660; YFP, 514/525–55.

Bimolecular fluorescence complementation

VYNE-LjRIN4, VYCE-LjCyPA, VYCE-LjCyPA^{F67A}, and *VYCE-LjCyPA*^{H133A} were generated in pENTR/D-TOPO using NEBuilder HiFi DNA Assembly (New England BioLabs, Hitchin, UK) and subsequently recombined into the modified Gateway binary vector proLjUBQ:GW-Hyg. *Agrobacterium tumefaciens* GV3101 harboring each split-Venus construct was coinfiltrated into *Nicotiana benthamiana* leaves, which were harvested 48 h later. Yellow fluorescent protein (YFP) fluorescence was observed using a confocal microscope (Zeiss LSM780), and its intensity was quantified from multiple cells using the ImageJ software.

Results

Identification of CyPA homologs in *Lotus japonicus*

A BLASTP analysis using canonical CyPAs (human CyPA and one of the Arabidopsis CyPAs, AtCYP18-3/ROC1) as queries identified three CyPA proteins in *L. japonicus*, which we named CyPA1 (Lj1g3v3343880), CyPA2 (Lj3g3v3527420), and CyPA3 (Lj3g3v3527430). These CyPAs shared highly conserved amino acid sequences with AtCYP18-3/ROC1: 92.4% (CyPA1), 92.4% (CyPA2), and 84.9% (CyPA3; Fig. S1a). AlphaFold2 prediction showed high structural similarity between AtCYP18-3/ROC1 and LjCyPAs with RMSD values of 0.083 Å (CyPA1), 0.106 Å (CyPA2), and 0.101 Å (CyPA3), and conservation of the residues in the active sites (Fig. S1b–d). *CyPA1* is located on Chromosome 1, whereas *CyPA2* and *CyPA3* are tandemly positioned on Chromosome 3 (Fig. 1a). According to our RNA-seq (Goto *et al.*, 2022), these mRNAs were abundant in both *Mesorhizobium loti*-inoculated and noninoculated roots in early-infection stage (0–3 DAI; Fig. S2).

CyPA1 facilitates intracellular root-hair entry of symbiotic bacteria

We utilized CRISPR technology to create knockout lines with nonsense mutations in *CyPA1*, *CyPA2*, and *CyPA3* genes of *L. japonicus* MG-20 WT (Fig. S3). Among these, *CyPA1* mutation had a significant impact on nodule symbiosis with the highly compatible rhizobium *M. loti* MAFF303099. The *LjcypA1* mutant plants showed a decrease in the number of normal ITs at 8 DAI compared with MG-20 WT and the other *LjcypA2* and *LjcypA3* mutant plants (Fig. 1b). The infection phenotype of *LjcypA1* was validated using an independent *LjcypA1* mutant (-*LjcypA1-2*; Fig. S4). Constitutive expression of *LjCyPA1* restored its transcripts and IT number in a hairy root transformation system (Fig. S5). Compared with the normal ITs in MG-20 (Fig. 1c), ITs in the *LjcypA1* mutant were frequently abnormal, with progression arrested at the initiation or elongation stage. Inside of these ITs, rhizobia did to organize into continuous thread-like arrangements and were fragmented, while the ITs themselves developed balloon-like swellings (Figs 1d–f, S6). When we examined the infection phenotypes at an earlier timepoint (5 DAI), the total number of ITs did not differ (Fig. 1g), but abnormal ITs were significantly more frequent in the *LjcypA1* mutant (Fig. 1h,i). These findings indicate that *LjCyPA1* serves ensuring effective IT progression within root hairs.

CyPA1 and rhizobial T3SS cooperate in rhizobial infection and nodulation

Rhizobia use T3SS to deliver effector proteins (T3Es) into the host cells to regulate symbiosis (Marie *et al.*, 2001; Miwa & Okazaki, 2017). To explore the relationship between LjCyPA1 and rhizobial T3Es during root-hair infection, we engineered a mutant of *M. loti* MAFF303099 lacking the T3SS genes (ΔT3SS; Fig. 2a; Table S1). At the early-infection stage (5 DAI), the *LjcypA1* mutant showed significantly reduced normal ITs but not total ITs after inoculation with the *M. loti* ΔT3SS mutant (Fig. 2b,c). Sixteen percent of ITs in MG-20 were abnormal following the *M. loti* ΔT3SS mutant inoculation, a slight increase from the 8% observed with *M. loti* MAFF303099 (Fig. 2d). By contrast, the *LjcypA1* mutant exhibited 53% abnormal ITs following the *M. loti* ΔT3SS mutant inoculation, a dramatic increase from the 21% observed with *M. loti* MAFF303099 (Fig. 2d).

In nodule organogenesis, there were morphological differences that could affect their maturity (Fig. 3). Brownish-white nodule primordia with black wounds were only observed in the *LjcypA1* mutant 2 wk after inoculation (Fig. 3b,d). This result showed that the *LjcypA1* mutant increased nodulation with abnormal morphology not only in epidermal infection. On the contrary, transgenic hairy roots showed individual loss of *CyPA1*, or inoculation with the *M. loti* ΔT3SS mutant did not affect nodule number; however, the simultaneous loss of both *CyPA1* and T3SS severely impaired nodule formation (Fig. 3e,f). These results indicate that host CyPA1 and rhizobial T3Es redundantly function in the compatible symbiosis.

CyPA1 and rhizobial T3SS affect immune and symbiotic expression

To investigate transcriptomic differences associated with host genotype (MG-20 vs the *LjcypA1* mutant) and plant responses to the *M. loti* ΔT3SS mutant (noninoculation vs 3 DAI), we conducted RNA sequencing. A total of 356 DEGs were identified (FDR < 0.05; Table S3), and those with a fold change > 2 were categorized as MG-20-specific, *LjcypA1*-specific, or shared DEGs

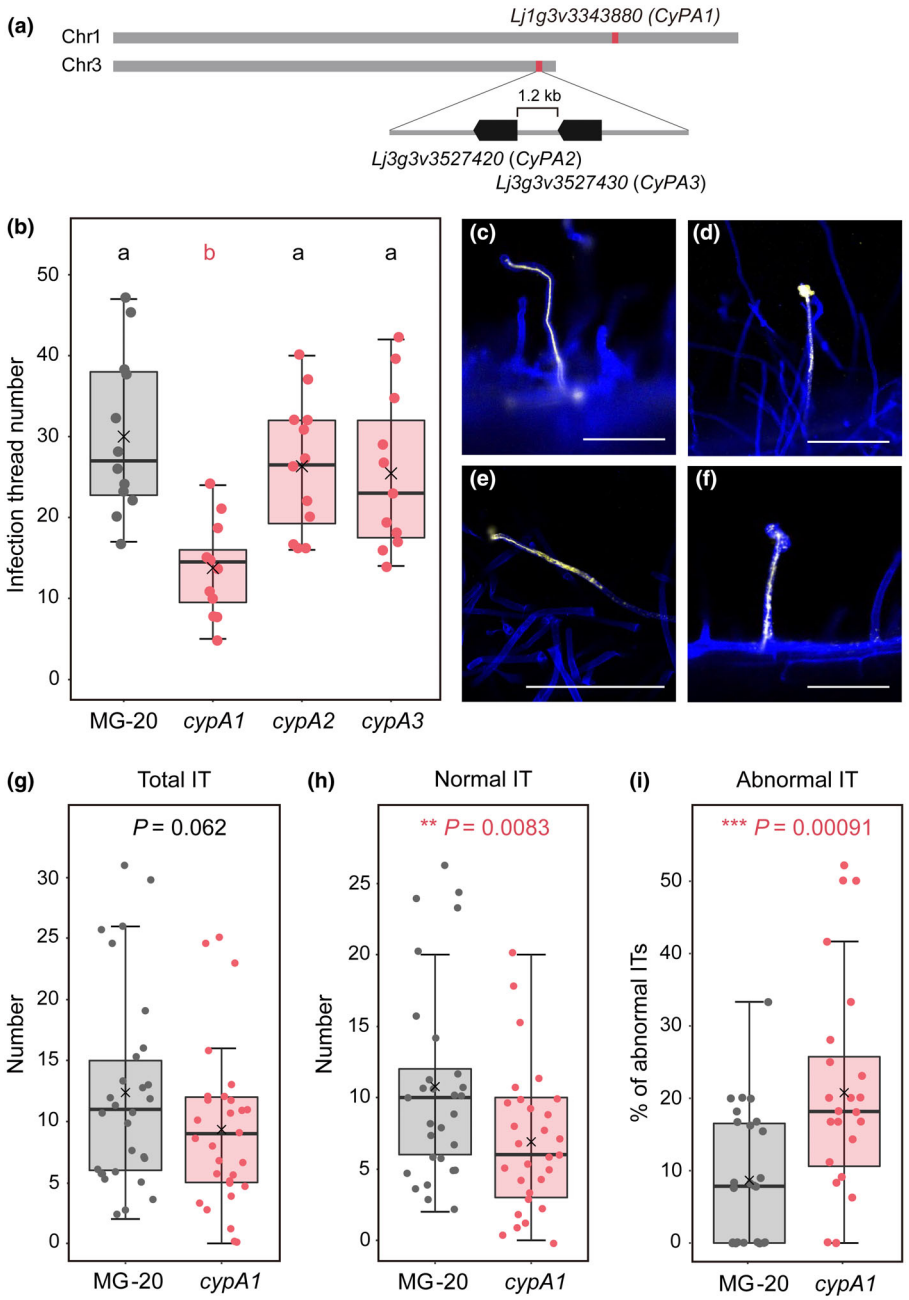

Fig. 1 *CypA1* ensures the process of rhizobial intracellular infection. (a) Genomic location of *CyPA1* (*Lj1g3v3343880*) on Chromosome 1, and *CyPA2* (*Lj3g3v3527420*), and *CyPA3* (*Lj3g3v3527430*) on Chromosome 3. (b) Number of infection threads (ITs) in MG-20 wild-type (WT), *cypA1*, *cypA2*, and *cypA3* mutants at 8 d after inoculation (DAI). ANOVA followed by Tukey's honestly significant difference (HSD) test ($P < 0.05$). Different letters indicate significant differences. (c–f) Representative phenotypes of normal ITs in MG20 WT (c) and abnormal ITs in the *cypA1* mutant (d–f) in each stage of IT elongation: initiation (d), middle elongation (e), or elongated ITs (f). Bar, 100 μm. (g–i) The number of total ITs (normal + abnormal) (g) and normal ITs (h), and the proportion of abnormal ITs (number of abnormal ITs/total ITs) (i) at 5 DAI. Asterisks indicate statistically significant differences as (g, h): Welch's *t*-test and (i) Fisher's exact test. In the boxplots, the horizontal line indicates the median, the box represents the interquartile range (IQR), whiskers extend to 1.5 × IQR. Each dot represents an individual data point. CyPA, *Lotus japonicus* Cyclophilin A.

(Fig. S7a). Hierarchical clustering based on expression dynamics before and after inoculation separated DEGs into five clusters (I–V; Fig. S7b), among which Clusters I–IV contained several resistance- and defense-related genes (Fig. S7c). qRT-PCR was then used to further compare expression patterns following noninoculation, *M. loti* MAFF303099 inoculation, and the *M. loti* Δ T3SS-inoculation in MG-20 and the *LjcypA1* mutant (Fig. S8). In MG-20 roots, the *Lotus* homolog of *RPS2* (*Lotja-Gi1g1v0088300*), an NBS-LRR class resistance gene known to suppress pathogen infection in *Arabidopsis* leaves (Bent *et al.*, 1994; Mindrinos *et al.*, 1994), was downregulated following inoculation with *M. loti* MAFF303099, but not with the *M.*

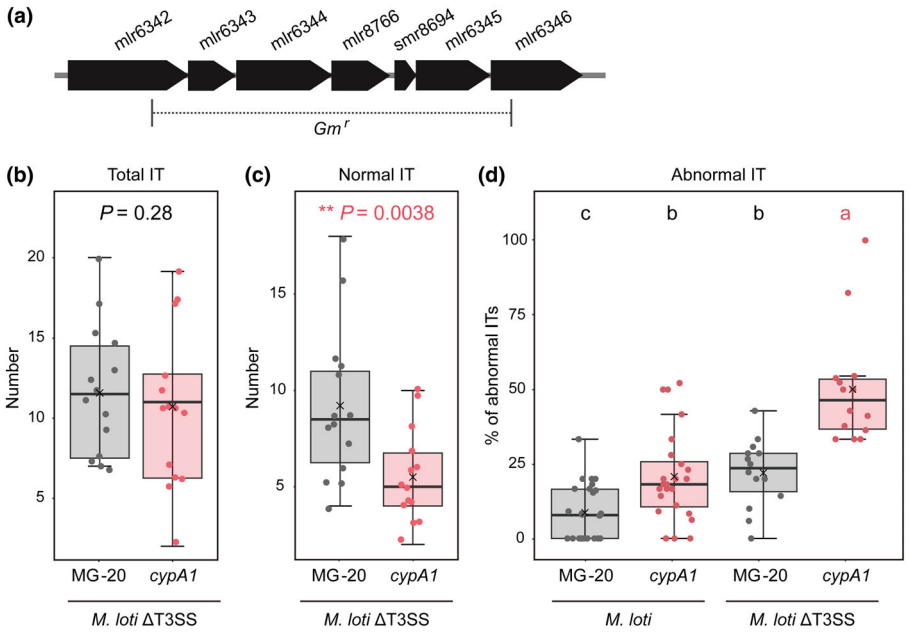

Fig. 2 CyPA1 and compatible rhizobial type III secretion system (T3SS) facilitate intracellular infection. (a) T3SS-deficient *Mesorhizobium loti* MAFF303099 (the *M. loti* ΔT3SS mutant). (b–d) The number of total ITs (normal + abnormal) (b) and normal ITs (c), and the percentage of abnormal ITs (number of abnormal ITs/total ITs) (d) at 5 d after inoculation with *M. loti* MAFF303099 or the *M. loti* ΔT3SS mutant. Asterisks and different letters indicate that differences are statistically significant as (b, c): Welch's *t*-test and (d) Fisher's exact test. In the boxplots, the horizontal line indicates the median, the box represents the interquartile range (IQR), whiskers extend to 1.5 × IQR. Each dot represents an individual data point. CyPA, *Lotus japonicus* Cyclophilin A.

loti ΔT3SS mutant. While in the *LjcypA1* mutant, no such down-regulation was observed with either mesorhizobial strain (Fig. S8). These results suggest that the expression of *RPS2* is modulated by both LjCyPA1 and rhizobial T3Es. By contrast, *Chitinase* genes (*LotjaGi5g1v0054800 and LotjaGi5g1v0055200*) were downregulated after inoculation with both mesorhizobial strains in MG-20, while its expression remained stable in the *LjcypA1* mutant (Fig. S8), indicating CyPA1-dependent but not T3E. Interestingly, when the *Ljcypa1* mutant was inoculated with the *M. loti* ΔT3SS mutant, a *Defensin-like* gene (*LotjaGi3g1v0086300_LC*) resulted in dramatic induction (Fig. S8), suggesting that CyPA1 and T3E components synergize in its expression. We also examined the expression pattern of several symbiotic genes. *ERN1*, a symbiotic *trans*cription factor for intracellular rhizobial infection (Cerri *et al.*, 2017; Yano *et al.*, 2017; Kawaharada *et al.*, 2017a; Montiel *et al.*, 2021), was not induced in the *cypA1* mutant upon inoculation with the *M. loti* ΔT3SS mutant (Fig. S8). Meanwhile, *RPG*, a regulator of polarized IT elongation (Arrighi *et al.*, 2008; Lace *et al.*, 2023; Li *et al.*, 2023), showed no significant induction after inoculation with the *M. loti* ΔT3SS mutant compared with *M. loti* MAFF303099 inoculation in MG-20 (Fig. S8). *NFR1*, whose expression is reduced following compatible rhizobia inoculation (Frank *et al.*, 2023), was also downregulated in the *LjcypA1* mutant when inoculated with both *M. loti* MAFF303099 and the *M. loti* ΔT3SS mutant (Fig. S8). Together, these results demonstrate that CyPA1 influences the expression of both immune-related and symbiotic genes involved in IT formation during the early stages of infection, through both T3E-dependent and T3E-independent mechanisms.

Gain-of-function CyPA1 enhances symbiosis with both compatible and incompatible rhizobia

A gain-of-function mutant of CyPA (*CyPA*^{S58F}; *roc1* mutation) was previously identified in Arabidopsis (Ma *et al.*, 2013), and has been shown to strongly suppress immunity against pathogens (Li *et al.*, 2014). To investigate whether a gain-of-function LjCyPA1 affects common signaling components also involved in the symbiotic nodulation, we examined the effect on intracellular infection and nodule formation. Constitutive expression of *LjCyPA1*^{S58F} significantly increases the number of ITs and nodules after inoculation with *M. loti* MAFF303099 compared with controls expressing either an empty vector or native *LjCyPA1* (Fig. 4a,b). When inoculated with the *M. loti* ΔT3SS mutant, *LjCyPA1*^{S58F} also promoted nodule formation, although to a lesser extent compared with when inoculated with *M. loti* MAFF303099 (Fig. S9).

Building on these findings, we explored whether the gain-of-function mutation alleviates severe symbiotic incompatibility caused by ETI. We focused on the interaction between the soybean cultivar Hardee and *Bradyrhizobium diazoefficiens* USDA122. The host R gene *Rj2* recognizes the incompatible NopP effector and triggers immunity (Fig. 4c; Sugawara *et al.*, 2018, 2019). In this incompatible *B. diazoefficiens* USDA122 inoculation, native *LjCyPA1* expression in Hardee could not promote nodulation, resulting in very few or no nodules (Fig. 4d). However, the gain-of-function *LjCyPA1*^{S58F} significantly promoted nodulation (Fig. 4d). Furthermore, NopP-deficient mutant (USDA122ΔnopP), which reverts to a

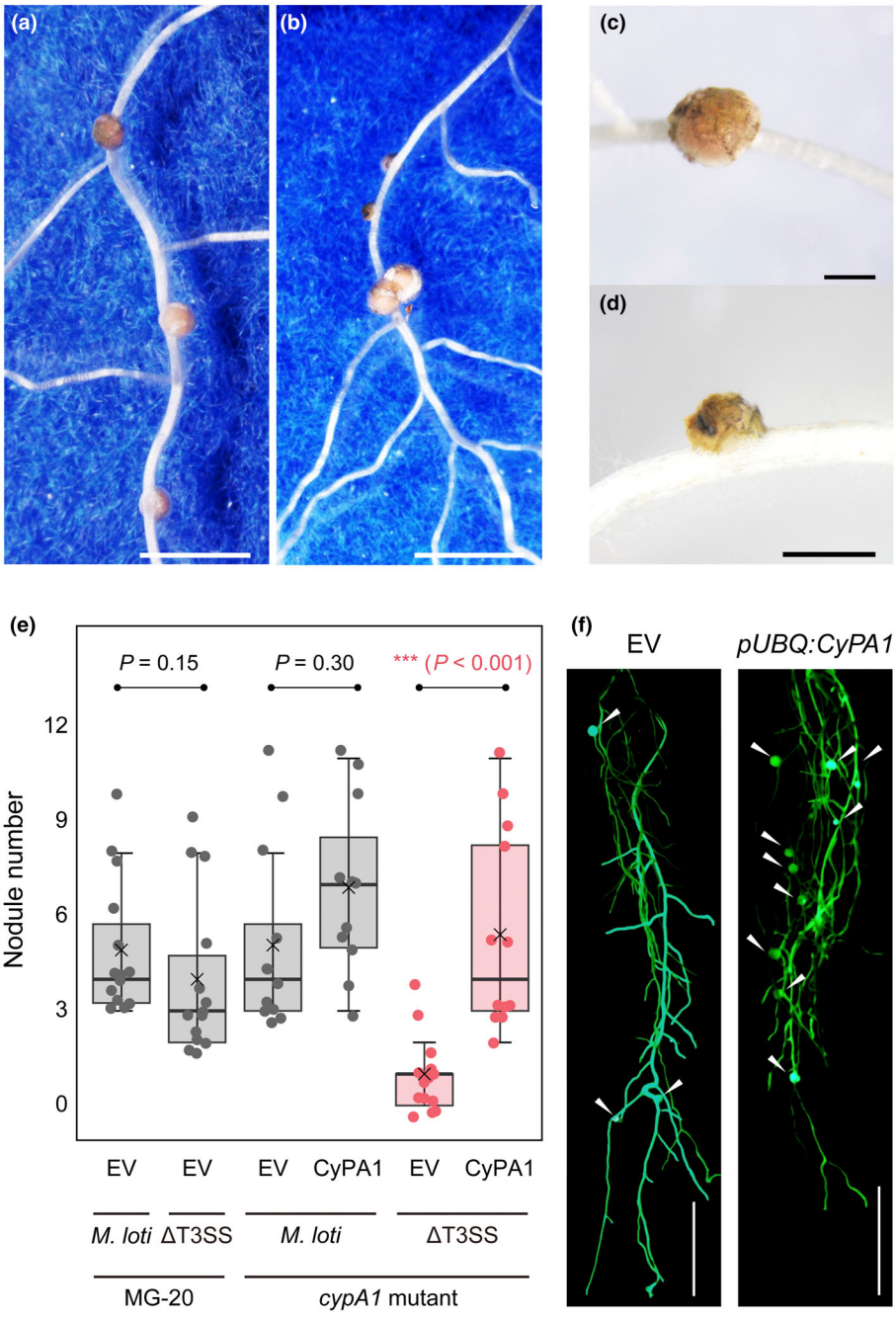

Fig. 3 Nodulation phenotypes in MG-20 and the *cypA1* mutant with the *Mesorhizobium loti* ΔT3SS mutant. (a, c) Nodules on MG-20 wild-type at 14 d after inoculation (DAI). (b, d) Brownish-white nodule primordia on the *cypA1* mutant at 14 DAI. Bars: 500 μm (a, b), 100 μm (c, d). (e) The nodule number in hairy roots of the *cypA1* mutants harboring empty vector (EV with green fluorescent (GFP)) and *pUBQ:CyPA1-GFP* vector 3 wk after inoculation. Asterisks indicate statistical difference by Welch's *t*-test. (f) Representative phenotype of hairy roots of *cypA1* mutants harboring EV (Left) and *pUBQ:CyPA1-GFP* vector (Right) with the *M. loti* ΔT3SS mutant. Nodules are indicated by arrowheads. Bar, 1 cm. In the boxplots, the horizontal line indicates the median, the box represents the interquartile range (IQR), whiskers extend to 1.5 × IQR. Each dot represents an individual data point. CyPA, *Lotus japonicus* Cyclophilin A; T3SS, type III secretion system.

compatible strain, showed high nodule formation with the gain-of-function $LjCyPA1^{S58F}$ expression roots (Fig. 4d), similar to *M. loti* MAFF303099 inoculation in $LjCyPA1^{S58F}$ variant in MG-20 (Fig. 4b). These results indicate that a gain-of-function of *LjCyPA1* promotes symbiotic nodulation regardless of host-rhizobia compatibility.

A *cis/trans* isomerization of RIN4 is required for root–hair infection

AtCYP18-3/ROC1 interacts with and catalyzes *cis/trans* isomerization of RIN4, a plant immune signaling hub (Li *et al.*, 2014). *L. japonicus* possesses a single LjRIN4 (Lj3g3v0730080) and our structural modeling predicted that LjCyPA1 forms a complex with an LjRIN4 peptide (182-KGAAVPKFGEWD-193), in which proline-187 interacts with the hydrophobic pocket of LjCyPA1 (Fig. 5a). In this model, a π–π stacking interaction between phenylalanine-67 of LjCyPA1 and phenylalanine-189 of LjRIN4 was predicted to be important for this binding (Fig. 5a). Additionally, histidine-133 of LjCyPA1 was expected to interact with proline-187 of LjRIN4 to facilitate its isomerization (Fig. 5a). To investigate the importance of these aromatic ring interactions, we replaced phenylalanine-67 with Alanine (F67A) or Histidine-133 with Alanine (H133A) in LjCyPA1. In

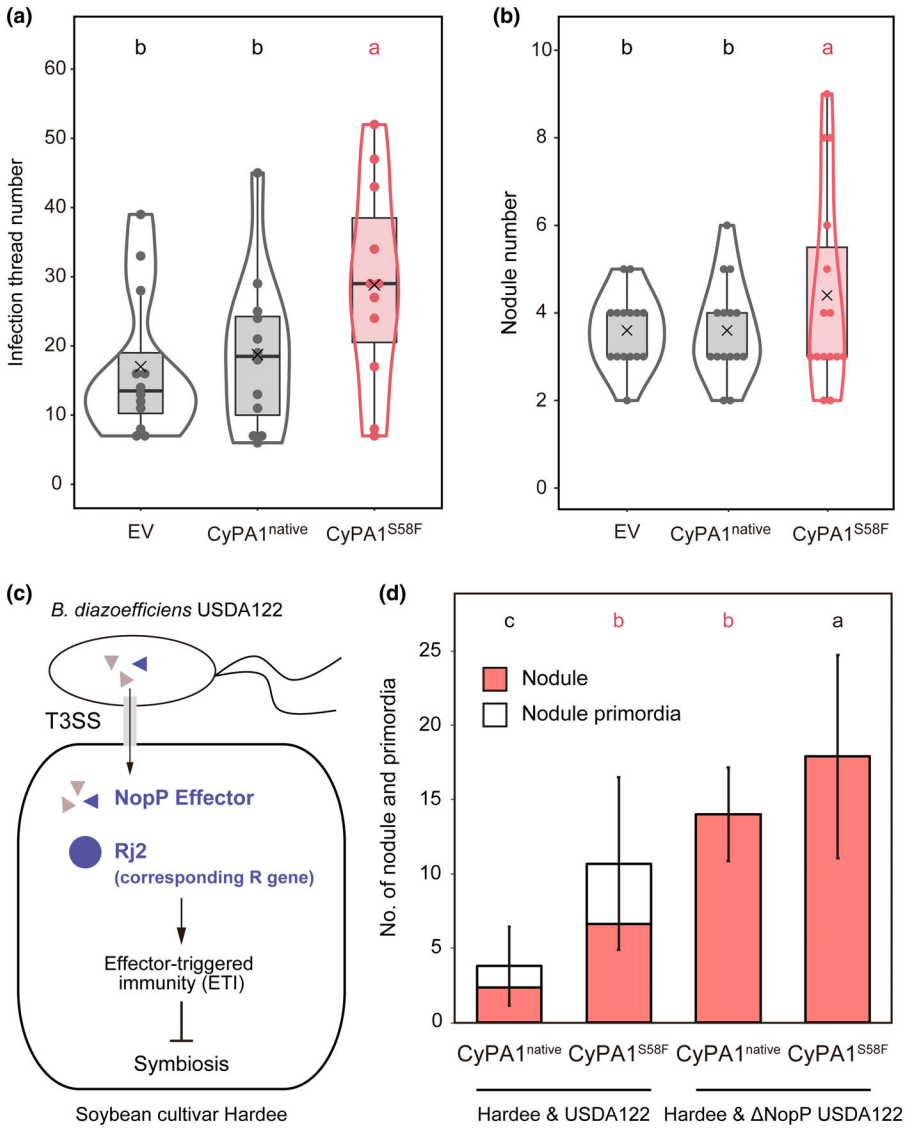

Fig. 4 Gain-of-function of *CyPA1* promotes symbiosis with both compatible and incompatible rhizobia. (a, b) The number of infection threads (a) and nodules (b) in hairy roots of MG-20 wild-type harboring empty vector (EV) (Control 1), *pUBQ:LjCyPA1-GFP* vector (Control 2), and *pUBQ:LjCyPA1*^{S58F}*-GFP* vector (gain-of-function). Infection threads and nodules were counted 2 and 3 wk after inoculation, respectively. (c) A schematic illustration of effector-triggered immunity (ETI) in interaction with incompatible *Bradyrhizobium diazoefficiens* USDA122 with soybean cultivar Hardee. Hardee's Rj2 recognizes NopP effector secreted by *B. diazoefficiens* USDA122 and activates ETI and suppresses nodule formation. (d) The number of nodules (pink) and primordia (white) in hairy roots of soybean cultivar Hardee with expressing *pUBQ:LjCyPA1-GFP* and *pUBQ:LjCyPA1*^{S58F}*-GFP*. Error bars indicate means ± SDs ($n > 10$ hairy roots). ANOVA followed by Tukey's HSD test ($P < 0.05$). Different letters indicate significant differences. In the boxplots, the horizontal line indicates the median, the box represents the interquartile range (IQR), whiskers extend to 1.5 × IQR. Each dot represents an individual data point. CyPA, *Lotus japonicus* Cyclophilin A.

bimolecular fluorescence complementation (BiFC) assays between LjCyPA1 and LjRIN4, LjCyPA1^{F67A} exhibited a weakened YFP signal compared with LjCyPA1 and LjCyPA1^{H133A} (Fig. S10). Regarding nodulation, neither LjCyPA1^{F67A} nor LjCyPA1^{H133A} could complement nodulation in the *LjcypA1* mutant (Fig. 5b). These results suggest that both binding to LjRIN4 and LjCyPA1-mediated isomerization are essential for nodule symbiosis. Furthermore, we investigated the impact of *cis*/*trans* isomerization of RIN4 on nodule symbiosis. Proline peptide bonds are naturally biased toward the *trans* form, but *cis*/*trans* isomerases increase the proportion of the *cis* form. We induced stable *cis* and *trans* isomers (LjRIN4$^{\Delta P187}$ and LjRIN4^{P187V}, respectively as described previously; Li *et al.*, 2014) in hairy roots of MG-20 and inoculated with *M. loti* MAFF303099. The LjRIN4$^{\Delta P187}$ *trans*genic roots promoted nodule and normal IT formation (Fig. 5c,d). By contrast, LjRIN4^{P187V} did not affect nodule formation but inhibited normal IT formation (Fig. 5c,d). The opposite phenotypes of RIN4$^{\Delta P187}$ and RIN4^{P187V} suggest that shifting the equilibrium from *trans* to *cis* is crucial for symbiosis. Interestingly, when

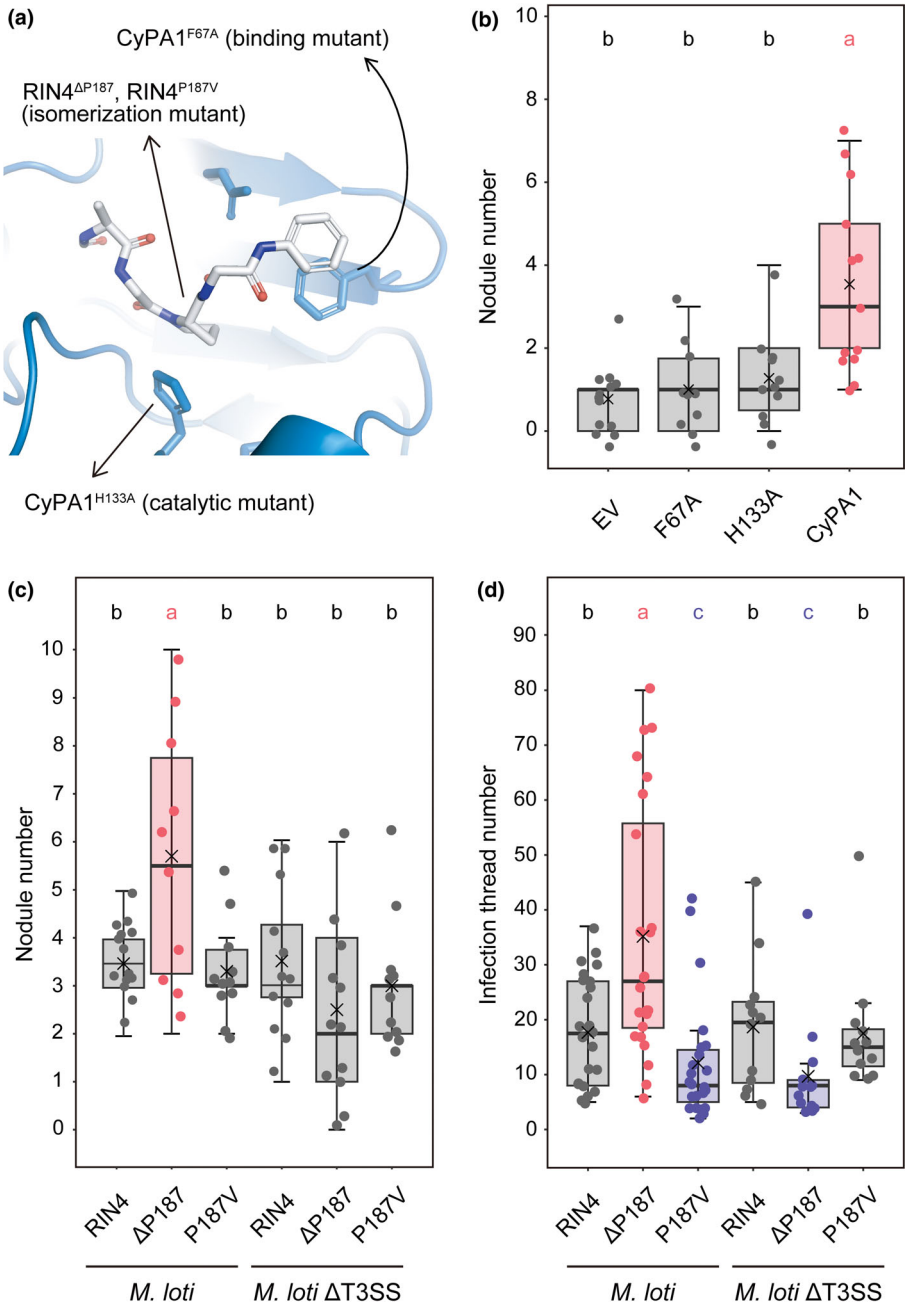

Fig. 5 Functional interaction between Cyclophilin A (CyPA) and RIN4 in *Lotus japonicus* nodule symbiosis. (a) Interaction sites between CyPA1 and RIN4 peptide (182-KGAAVPKFGEWD-193) *in silico*. (b) The nodule number in hairy roots of *cypA1* mutants harboring empty vector (EV) (negative control), *pUBQ:LjCyPA1*^{F67A}*-GFP* vector (binding mutant), *pUBQ:LjCyPA1*^{H133A}*-GFP* vector (catalytic mutant), and *pUBQ:LjCyPA1-GFP* vector (positive control), 3 wk after inoculation with the *Mesorhizobium loti* ΔT3SS mutant. (c, d) The number of nodules (c) and infection threads (d) in hairy roots of MG-20 with constitutive expression of RIN4 (control), RIN4$^{\Delta P187}$ (*cis* conformer), and RIN4^{P187V} (*trans* conformer). Infection threads and nodules were counted 2 and 3 wk after inoculation with *M. loti* MAFF303099 or the *M. loti* ΔT3SS mutant, respectively. ANOVA followed by Tukey's HSD test ($P < 0.05$). Different letters indicate significant differences. In the boxplots, the horizontal line indicates the median, the box represents the interquartile range (IQR), whiskers extend to 1.5 × IQR. Each dot represents an individual data point. T3SS, type III secretion system.

inoculated with the *M. loti* ΔT3SS mutant, RIN4$^{\Delta P187}$ did not promote normal IT and nodule formation (Fig. 5c,d). These findings indicate that unknown T3Es in *M. loti* MAFFF303099 are required for promoting symbiosis, working in coordination with the *cis/trans* isomerization at proline-187 of LjRIN4.

Loss of CyPA1 correlates with absence of intracellular infection in basal legumes

To investigate the evolutionary conservation of the *CyPA1*-mediated control of intracellular infection, we performed a genome-wide analysis of legumes and nonlegumes. Previous phylogenetic analysis has shown that plant CyPs have undergone repeated duplications (Singh *et al.*, 2020); however, the evolutionary trajectory of specific CyPAs has not been examined. We performed a synteny analysis of the genomic regions surrounding LjCyPA1 orthologs loci in legumes and nonlegumes with high-quality genomes. LjCyPA1 orthologs were well conserved in nonlegumes as well as legumes (Fig. 6). However, notably, LjCyPA1 orthologs were absent in some early-branching legume genera, such as *Lupinus* (*albus*, *angustifolius*) and *Arachis* (*duranensis*, *ipaensis*) that do not form intracellular ITs (Fig. 6), suggesting the evolutionary loss of CyPA1 in these genera. As an exception, another basal legume *Aeschynomene evenia* possesses a *CyPA1* ortholog, suggesting that CyPA1 was independently lost in the *Lupinus* and *Arachis* genera (Fig. 6). By contrast, LjCyPA2/CyPA3 orthologs were conserved in those species (Fig. S11). These data demonstrate an evolutionary link between

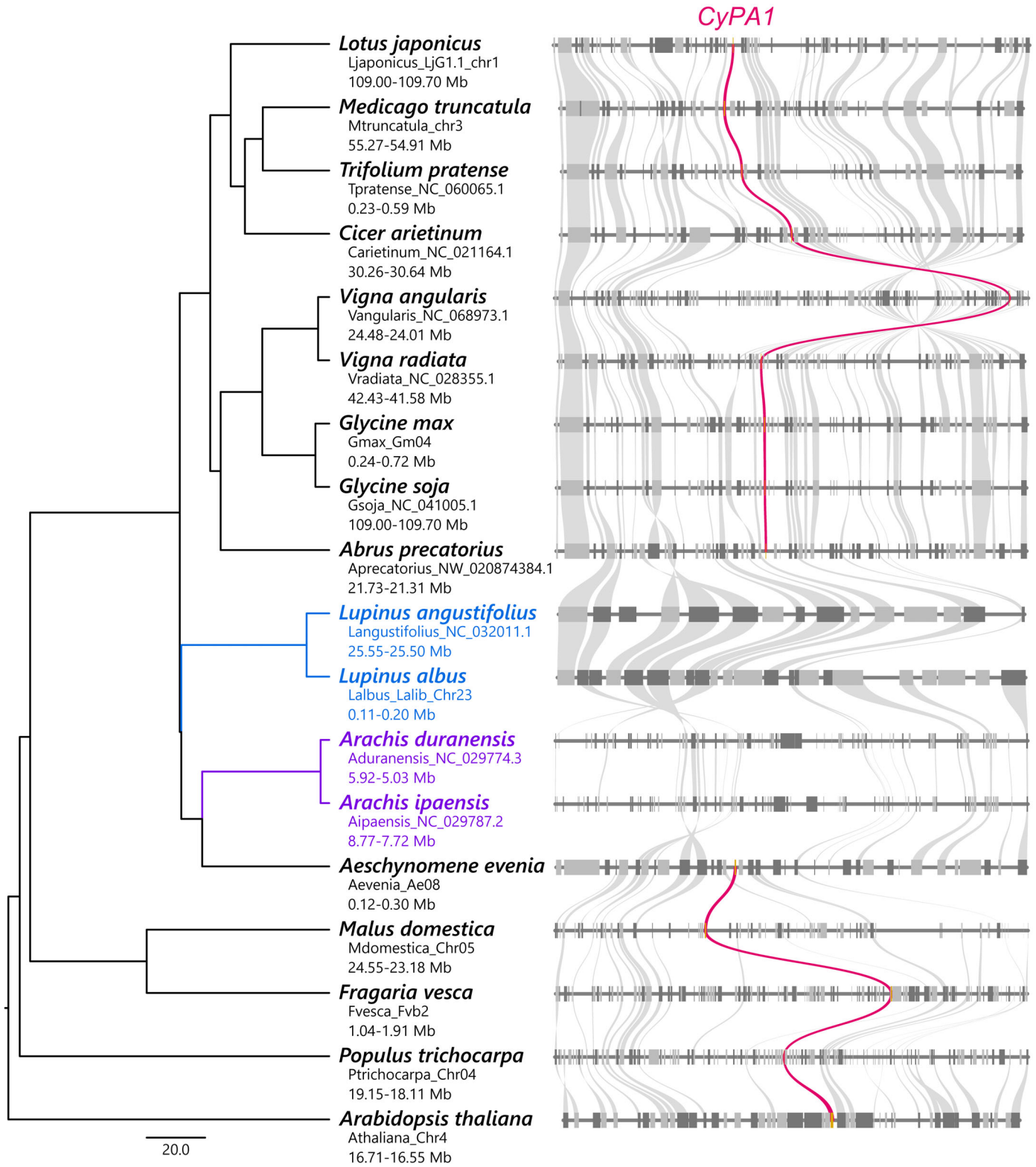

Fig. 6 Cyclophilin A (*CyPA1*) conservation in representative legumes and nonlegumes. Orthologous genes in each specific block are connected by lines of gray or pink colors. *CyPA1* ortholog is highlighted in pink. Dark gray represents genes on the minus strand, while light gray represents genes on the plus strand. The phylogenetic tree to the left of the synteny blocks was obtained from TimeTree5, with the bar indicating divergence time in million years ago (Ma). The following plant species were included in this analysis: *Lotus japonicus*, *Medicago truncatula*, *Trifolium pratense*, *Cicer arietinum*, *Glycine max*, *Glycine soja*, *Vigna angularis*, *Vigna radiata*, *Abrus precatorius*, *Arachis ipaensis*, *Arachis duranensis*, *Lupinus albus*, *Lupinus angustifolius*, *Aeschynomene evenia*, *Fragaria vesca*, *Malus domestica*, *Populus trichocarpa*, and *Arabidopsis thaliana*.

CyPA1 and symbiotic traits and suggest that *CyPA1* is evolutionarily important for intracellular infection in legumes that develop ITs.

Discussion

Among post-*trans*lational modifications, peptidyl-prolyl *cis/trans* isomerization is a universal process that alters protein conformation that can switch the direction of signaling. A wide range of studies, including structural biology and reaction kinetics, have underscored the importance of CyPs in catalyzing this isomerization (Li & Cui, 2003; Fanghänel & Fischer, 2004; Lu *et al.*, 2007; Hamelberg & McCammon, 2009; Jakob & Schmid, 2009; Camilloni *et al.*, 2014). One of the CyPs, CyPA, has been extensively studied in animals since its discovery as a binding protein for the immunosuppressive drug (Handschumacher *et al.*, 1984). By contrast, the plant CyPA has undergone duplication and diversification, limiting our understanding of its physiological function (Singh *et al.*, 2020). A decade ago, forward genetics in Arabidopsis led to the identification of *roc1*, a gain-of-function mutant of one of the CyPAs, shedding light on the *cis/trans* isomerization in plants. Subsequent studies revealed that AtCYP18-3/ROC1 catalyzes the *cis/trans* isomerization of RIN4, a key signaling hub in plant immunity (Li *et al.*, 2014). However, it remained a puzzling aspect of plant–microbe interactions how CyPA plays a paradoxical role in suppressing host immunity against pathogens. In this study, we investigated the role of CyPA in the context of root nodule symbiosis. We found that *LjCyPA1*, one of the *L. japonicus CyPAs*, has a native function in facilitating intracellular infection of compatible rhizobia (Figs 1, 2, S4). A gain-of-function variant, LjCyPA1^{S58F}, accelerated symbiosis even with otherwise incompatible *B. diazoefficiens* USDA122 in a soybean cultivar Hardee (Fig. 4d), highlighting the importance of *cis/trans* isomerization for the proper regulation of host immune responses.

Phenotypic analysis combined with structural modeling supports the functional importance of the association between LjCyPA and LjRIN4 in nodule symbiosis (Figs 5a,b, S10). Engineered stable *cis* and *trans* conformers of LjRIN4 at Proline-187 induced opposite phenotypes (Fig. 5c,d), indicating that RIN4's conformational state plays a role in determining the acceptance of symbionts. Interestingly, this effect depends on the presence of T3SS in *M. loti* MAFF303099, as the promotion of infection through *cis* isomerization at Proline-187 was observed only when unknown T3Es were present (Fig. 5c,d). On the contrary, LjCyPA1 and T3SS exhibit synergistic effects on infection and nodulation, as their simultaneous loss of both causes a stronger phenotypic effect than the loss of either one alone (Figs 2, 3). Together, these results suggest that LjCyPA1 promotes rhizobial infection through two distinct mechanisms: one involves a T3E-independent pathway, such as down-regulation of *Chitinase* (Fig. S8). The other involves LjCyPA1 acting on *cis* isomerization of LjRIN4, which requires compatible rhizobial T3Es for its function (Fig. 5c,d). This function was supported by *RPS2* and *Defensin-like* expression patterns (Fig. S8). Thus, while CyPA1 and T3Es act synergistically at the overall level, a hierarchical relationship exists in which T3E-dependent regulation occurs at the level of specific targets. Previous studies of the plant immune system have shown that various pathogenic T3Es, such as AvrRpm1, AvrB, AvrRpt2, HopF2, and HopZ3, directly interact with RIN4 (Mackey *et al.*, 2002, 2003; Axtell & Staskawicz, 2003; Wilton *et al.*, 2010; Lee *et al.*, 2015). Among them, AvrRpm1 and AvrB effectors phosphorylate AtRIN4 and activate RPM1-mediated defense response (Mackey *et al.*, 2002). Also, a novel phosphorylation site of RIN4, unique to the nitrogen-fixing clade, has been recently identified as essential for nodule symbiosis (Tóth *et al.*, 2023). Given these findings, both *cis/trans* isomerization by CyPA1 and phosphorylation by unknown T3Es from compatible rhizobia may alter RIN4 conformation, influencing symbiosis. Understanding how RIN4 adopts distinct conformational states under various microbial influences will be an important direction for future research. RIN4 may serve as a molecular switch integrating symbiotic and immune signals via multiple post-translational modifications.

Given that the evolutionary robustness of the intracellular infection system is linked to the CyPA1 ortholog conservation in legumes (Fig. 6), the biological significance of CyPA1's function in balancing the immune response may be related to the advantage of intracellular infection in legumes. Intracellular infection via ITs represents a 'closed' infection system and is superior in that legume actively recruits compatible rhizobia while modulating immunity to avoid rejection. This study demonstrates that LjCyPA1 serves a fundamental role in this pathway by preventing IT abortion during elongation (Fig. 1). Early-branching legumes that do not provide ITs have lost CyPA1 (Fig. 6), which may reflect evolutionary pressures to mitigate risks, such as hijacking of root hairs by a pathogen. Alternatively, in these lineages, the CyPA1 loss may have gradually weakened the dominance of the IT strategy, eventually leading to the loss of ITs. Despite high sequence and structure conservation among *LjCyPAs* (Fig. S1), only *LjCyPA1* appears functionally essential for the symbiosis. This functional divergence could not be explained by expression patterns (Frank *et al.*, 2023), suggesting that unidentified sequence variations may underlie their functional diversification. Our study provides key insights into how CyPA1-mediated *cis/trans* isomerization balances the immune response, ensuring robust symbiotic interactions.

Acknowledgements

We thank Ms. Sachiko Tanaka (National Institute for Basic Biology; NIBB) and Dr Kamolchanok Umnajkitikorn (Suranaree University of Technology) for their technical suggestions. We also thank Dr Mitsutaka Fukudome (Kagoshima University), Dr Jesús Montiel (Universidad Nacional Autónoma de México), Dr Simona Radutoiu (Aarhus University), Dr Stig Uggerhøj Andersen (Aarhus University), Dr Johan Quilbé (Aarhus University), and Dr Aleksandr Gavrin (Aarhus University) for constructive discussions. This work was supported by the Optics and Imaging Facility (NIBB), the Data Integration and Analysis Facility (NIBB), the Grants-in-Aid for Scientific Research (23K19376), and the JSPS Overseas Research Fellowship (202460148).

Competing interests

None declared.

Author contributions

TG conceived the project. TG, YK and KRA designed the experiments. YK created the ΔT3SS mutant of *M. loti* MAFF303099. KRA conducted the structural analysis of CyPA1 and RIN4. TG and MB performed the synteny analysis. TG performed all other experiments. KM and MS provided the soybean cultivar Hardee, as well as *B. diazoefficiens* USDA122 and its *ΔnopP* mutant. MK and JS provided the experimental environments. TG and YK wrote the manuscript with feedback from KRA, SS, MK and JS.

ORCID

Kasper Røjkjær Andersen https://orcid.org/0000-0002-4415-8067
Masaru Bamba https://orcid.org/0000-0002-1486-7524
Takashi Goto https://orcid.org/0000-0002-2154-3042
Masayoshi Kawaguchi https://orcid.org/0000-0002-1032-6261
Yasuyuki Kawaharada https://orcid.org/0000-0002-4756-4394
Kiwamu Minamisawa https://orcid.org/0000-0001-7302-4079
Shusei Sato https://orcid.org/0000-0002-0293-5366
Jens Stougaard https://orcid.org/0000-0002-9312-2685
Masayuki Sugawara https://orcid.org/0000-0002-3058-4348

Data availability

Gene IDs and expression data are provided in the main text and Supporting Information (Table S1 and Table S3). RNA sequence data in this article have been deposited in the DDBJ Sequence Read Archive (accession no.: DRA026025).

References

Acosta-Jurado S, Rodríguez-Navarro D-N, Kawaharada Y, Rodríguez-Carvajal MA, Gil-Serrano A, Soria-Díaz ME, Pérez-Montaño F, Fernández-Perea J, Niu Y, Alias-Villegas C *et al.* 2019. Sinorhizobium fredii HH103 nolR and nodD2 mutants gain capacity for infection thread invasion of *Lotus japonicus* Gifu and *Lotus burttii*. *Environmental Microbiology* **21**: 1718–1739.

Arrighi J-F, Godfroy O, de Billy F, Saurat O, Jauneau A, Gough C. 2008. The RPG gene of *Medicago truncatula* controls Rhizobium-directed polar growth during infection. *Proceedings of the National Academy of Sciences, USA* **105**: 9817–9822.

Axtell MJ, Staskawicz BJ. 2003. Initiation of RPS2-specified disease resistance in Arabidopsis is coupled to the AvrRpt2-directed elimination of RIN4. *Cell* **112**: 369–377.

Becker A, Schmidt M, Jäger W, Pühler A. 1995. New gentamicin-resistance and lacZ promoter-probe cassettes suitable for insertion mutagenesis and generation of transcriptional fusions. *Gene* **162**: 37–39.

Bent AF, Kunkel BN, Dahlbeck D, Brown KL, Schmidt R, Giraudat J, Leung J, Staskawicz BJ. 1994. RPS2 of *Arabidopsis thaliana*: a leucine-rich repeat class of plant disease resistance genes. *Science* **265**: 1856–1860.

Broghammer A, Krusell L, Blaise M, Sauer J, Sullivan JT, Maolanon N, Vinther M, Lorentzen A, Madsen EB, Jensen KJ *et al.* 2012. Legume receptors perceive the rhizobial lipochitin oligosaccharide signal molecules by direct binding. *Proceedings of the National Academy of Sciences, USA* **109**: 13859–13864.

Camilloni C, Sahakyan AB, Holliday MJ, Isern NG, Zhang F, Eisenmesser EZ, Vendruscolo M. 2014. Cyclophilin A catalyzes proline isomerization by an electrostatic handle mechanism. *Proceedings of the National Academy of Sciences, USA* **111**: 10203–10208.

Cao Y, Halane MK, Gassmann W, Stacey G. 2017. The role of plant innate immunity in the legume-rhizobium symbiosis. *Annual Review of Plant Biology* **68**: 535–561.

Cerri MR, Wang Q, Stolz P, Folgmann J, Frances L, Katzer K, Li X, Heckmann AB, Wang TL, Downie JA *et al.* 2017. The ERN1 transcription factor gene is a target of the CCaMK/CYCLOPS complex and controls rhizobial infection in *Lotus japonicus*. *New Phytologist* **215**: 323–337.

Cole MA, Elkan GH. 1973. Transmissible resistance to Penicillin G, Neomycin, and Chloramphenicol in *Rhizobium japonicum*. *Antimicrobial Agents and Chemotherapy* **4**: 248–253.

Fanghänel J, Fischer G. 2004. Insights into the catalytic mechanism of peptidyl prolyl *cis/trans* isomerases. *FBL* **9**: 3453–3478.

Feng Y, Wu P, Liu C, Peng L, Wang T, Wang C, Tan Q, Li B, Ou Y, Zhu H *et al.* 2021. Suppression of LjBAK1-mediated immunity by SymRK promotes rhizobial infection in *Lotus japonicus*. *Molecular Plant* **14**: 1935–1950.

Finan TM, Kunkel B, Signer ER. 1986. Second symbiotic megaplasmid in *Rhizobium meliloti* carrying exopolysaccharide and thiamine synthesis genes. *Journal of Bacteriology* **167**: 66–72.

Frank M, Fechete LI, Tedeschi F, Nadzieja M, Nørgaard MMM, Montiel J, Andersen KR, Schierup MH, Reid D, Andersen SU. 2023. Single-cell analysis identifies genes facilitating rhizobium infection in *Lotus japonicus*. *Nature Communications* **14**: 7171.

Goto T, Soyano T, Liu M, Mori T, Kawaguchi M. 2022. Auxin methylation by IAMT1, duplicated in the legume lineage, promotes root nodule development in *Lotus japonicus*. *Proceedings of the National Academy of Sciences, USA* **119**: e2116549119.

Hamelberg D, McCammon JA. 2009. Mechanistic insight into the role of transition-state stabilization in Cyclophilin A. *Journal of the American Chemical Society* **131**: 147–152.

Handschumacher RE, Harding MW, Rice J, Drugge RJ, Speicher DW. 1984. Cyclophilin: a specific cytosolic binding protein for Cyclosporin A. *Science* **226**: 544–547.

Indrasumunar A, Kereszt A, Searle I, Miyagi M, Li D, Nguyen CDT, Men A, Carroll BJ, Gresshoff PM. 2010. Inactivation of duplicated nod factor receptor 5 (NFR5) genes in recessive loss-of-function non-nodulation mutants of allotetraploid soybean (*Glycine max* L. Merr.). *Plant and Cell Physiology* **51**: 201–214.

Indrasumunar A, Searle I, Lin M-H, Kereszt A, Men A, Carroll BJ, Gresshoff PM. 2011. Nodulation factor receptor kinase 1α controls nodule organ number in soybean (*Glycine max* L. Merr). *The Plant Journal* **65**: 39–50.

Ito Y, Nishizawa-Yokoi A, Endo M, Mikami M, Toki S. 2015. CRISPR/Cas9-mediated mutagenesis of the RIN locus that regulates tomato fruit ripening. *Biochemical and Biophysical Research Communications* **467**: 76–82.

Jakob RP, Schmid FX. 2009. Molecular determinants of a native-state prolyl isomerization. *Journal of Molecular Biology* **387**: 1017–1031.

Jones JDG, Dangl JL. 2006. The plant immune system. *Nature* **444**: 323–329.

Kawaharada Y, James EK, Kelly S, Sandal N, Stougaard J. 2017a. The ethylene responsive factor required for nodulation 1 (ERN1) transcription factor is required for infection-thread formation in *Lotus japonicus*. *Molecular Plant Microbe Interactions* **30**: 194–204.

Kawaharada Y, Kelly S, Nielsen MW, Hjuler CT, Gysel K, Muszyński A, Carlson RW, Thygesen MB, Sandal N, Asmussen MH *et al.* 2015. Receptor-mediated exopolysaccharide perception controls bacterial infection. *Nature* **523**: 308–312.

Kawaharada Y, Nielsen MW, Kelly S, James EK, Andersen KR, Rasmussen SR, Füchtbauer W, Madsen LH, Heckmann AB, Radutoiu S *et al.* 2017b. Differential regulation of the Epr3 receptor coordinates membrane-restricted rhizobial colonization of root nodule primordia. *Nature Communications* **8**: 14534.

Kelly S, Hansen SB, Rübsam H, Saake P, Pedersen EB, Gysel K, Madland E, Wu S, Wawra S, Reid D *et al.* 2023. A glycan receptor kinase facilitates intracellular accommodation of arbuscular mycorrhiza and symbiotic rhizobia in the legume *Lotus japonicus*. *PLoS Biology* **21**: e3002127.

Lace B, Su C, Perez DI, Rodriguez-Franco M, Vernié T, Batzenschlager M, Egli S, Liu CW, Ott T. 2023. RPG acts as a central determinant for infectosome formation and cellular polarization during intracellular rhizobial infections. *eLife* **12**: 159.

Lee J, Manning AJ, Wolfgeher D, Jelenska J, Cavanaugh KA, Xu H, Fernandez SM, Michelmore RW, Kron SJ, Greenberg JT. 2015. Acetylation of an NB-LRR plant immune-effector complex suppresses immunity. *Cell Reports* **13**: 1670–1682.

Lei Y, Lu L, Liu H-Y, Li S, Xing F, Chen L-L. 2014. CRISPR-P: a web tool for synthetic single-guide RNA design of CRISPR-system in plants. *Molecular Plant* **7**: 1494–1496.

Li G, Cui Q. 2003. What is so special about Arg 55 in the catalysis of Cyclophilin A? insights from hybrid QM/MM simulations. *Journal of the American Chemical Society* **125**: 15028–15038.

Li M, Ma X, Chiang Y-H, Yadeta KA, Ding P, Dong L, Zhao Y, Li X, Yu Y, Zhang L *et al.* 2014. Proline isomerization of the immune receptor-interacting protein RIN4 by a Cyclophilin inhibits effector-triggered immunity in Arabidopsis. *Cell Host & Microbe* **16**: 473–483.

Li X, Liu M, Cai M, Chiasson D, Groth M, Heckmann AB, Wang TL, Parniske M, Allan Downie J, Xie F. 2023. RPG interacts with E3-ligase CERBERUS to mediate rhizobial infection in *Lotus japonicus*. *PLoS Genetics* **19**: 159.

Liang Y, Cao Y, Tanaka K, Thibivilliers S, Wan J, Choi J, Kang C, Qiu J, Stacey G. 2013. Nonlegumes respond to rhizobial nod factors by suppressing the innate immune response. *Science* **341**: 1384–1387.

Limpens E, Franken C, Smit P, Willemse J, Bisseling T, Geurts R. 2003. LysM domain receptor kinases regulating rhizobial nod factor-induced infection. *Science* **302**: 630–633.

López-Lara IM, Blok-Tip L, Quinto C, Garcia ML, Stacey G, Bloemberg GV, Lamers GEM, Lugtenberg BJJ, Thomas-Oates JE, Spaink HP. 1996. NodZ of Bradyrhizobium extends the nodulation host range of Rhizobium by adding a fucosyl residue to nodulation signals. *Molecular Microbiology* **21**: 397–408.

Lu KP, Finn G, Lee TH, Nicholson LK. 2007. Prolyl *cis-trans* isomerization as a molecular timer. *Nature Chemical Biology* **3**: 619–629.

Ma C, Wang J, Gao Y, Dong X, Feng H, Yang M, Yu Y, Liu C, Wu X, Qi Z *et al.* 2024. The type III effector NopL interacts with GmREM1a and GmNFR5 to promote symbiosis in soybean. *Nature Communications* **15**: 498.

Ma X, Song L, Yang Y, Liu D. 2013. A gain-of-function mutation in the ROC1 gene alters plant architecture in Arabidopsis. *New Phytologist* **197**: 751–762.

Mackey D, Belkhadir Y, Alonso JM, Ecker JR, Dangl JL. 2003. *Arabidopsis* RIN4 is a target of the Type III virulence effector AvrRpt2 and modulates RPS2-mediated resistance. *Cell* **112**: 379–389.

Mackey D, Holt BF III, Wiig A, Dangl JL. 2002. RIN4 interacts with *Pseudomonas syringae* Type III effector molecules and is required for RPM1-mediated resistance in *Arabidopsis*. *Cell* **108**: 743–754.

Madsen EB, Madsen LH, Radutoiu S, Olbryt M, Rakwalska M, Szczyglowski K, Sato S, Kaneko T, Tabata S, Sandal N *et al.* 2003. A receptor kinase gene of the LysM type is involved in legume perception of rhizobial signals. *Nature* **425**: 637–640.

Madsen LH, Tirichine L, Jurkiewicz A, Sullivan JT, Heckmann AB, Bek AS, Ronson CW, James EK, Stougaard J. 2010. The molecular network governing nodule organogenesis and infection in the model legume *Lotus japonicus*. *Nature Communications* **1**: 10.

Marie C, Broughton WJ, Deakin WJ. 2001. Rhizobium type III secretion systems: legume charmers or alarmers? *Current Opinion in Plant Biology* **4**: 336–342.

Mindrinos M, Katagiri F, Yu G-L, Ausubel FM. 1994. The *A. thaliana* disease resistance gene RPS2 encodes a protein containing a nucleotide-binding site and leucine-rich repeats. *Cell* **78**: 1089–1099.

Miwa H, Okazaki S. 2017. How effectors promote beneficial interactions. *Current Opinion in Plant Biology* **38**: 148–154.

Montiel J, Reid D, Grønbæk TH, Benfeldt CM, James EK, Ott T, Ditengou FA, Nadzieja M, Kelly S, Stougaard J. 2021. Distinct signaling routes mediate intercellular and intracellular rhizobial infection in *Lotus japonicus*. *Plant Physiology* **185**: 1131–1147.

Okazaki S, Okabe S, Higashi M, Shimoda Y, Sato S, Tabata S, Hashiguchi M, Akashi R, Göttfert M, Saeki K. 2010. Identification and functional analysis of Type III effector proteins in *Mesorhizobium loti*. *MPMI* **23**: 223–234.

Piromyou P, Nguyen HP, Songwattana P, Boonchuen P, Teamtisong K, Tittabutr P, Boonkerd N, Alisha Tantasawat P, Göttfert M, Okazaki S *et al.* 2021. The Bradyrhizobium diazoefficiens type III effector NopE modulates the regulation of plant hormones towards nodulation in *Vigna radiata*. *Scientific Reports* **11**: 16604.

Quilbé J, Montiel J, Arrighi J-F, Stougaard J. 2022. Molecular mechanisms of intercellular rhizobial infection: novel findings of an ancient process. *Frontiers in Plant Science* **13**: 426.

Radutoiu S, Madsen LH, Madsen EB, Felle HH, Umehara Y, Grønlund M, Sato S, Nakamura Y, Tabata S, Sandal N *et al.* 2003. Plant recognition of symbiotic bacteria requires two LysM receptor-like kinases. *Nature* **425**: 585–592.

Radutoiu S, Madsen LH, Madsen EB, Jurkiewicz A, Fukai E, Quistgaard EMH, Albrektsen AS, James EK, Thirup S, Stougaard J. 2007. LysM domains mediate lipochitin oligosaccharide recognition and *Nfr* genes extend the symbiotic host range. *EMBO Journal* **26**: 3923–3935.

Ray SK, Macoy DM, Kim W-Y, Lee SY, Kim MG. 2019. Role of RIN4 in regulating PAMP-triggered immunity and effector-triggered immunity: current status and future perspectives. *Molecules and Cells* **42**: 503–511.

Rey T, André O, Nars A, Dumas B, Gough C, Bottin A, Jacquet C. 2019. Lipo-chitooligosaccharide signalling blocks a rapid pathogen-induced ROS burst without impeding immunity. *New Phytologist* **221**: 743–749.

Roche P, Maillet F, Plazanet C, Debellé F, Ferro M, Truchet G, Promé J-C, Dénarié J. 1996. The common nodABC genes of Rhizobium meliloti are host-range determinants. *Proceedings of the National Academy of Sciences, USA* **93**: 15305–15310.

Shaw SL, Long SR. 2003. Nod factor inhibition of reactive oxygen efflux in a host legume. *Plant Physiology* **132**: 2196–2204.

Singh H, Kaur K, Singh M, Kaur G, Singh P. 2020. Plant cyclophilins: multifaceted proteins with versatile roles. *Frontiers in Plant Science* **11**: 128.

Skorupska A, Janczarek M, Marczak M, Mazur A, Król J. 2006. Rhizobial exopolysaccharides: genetic control and symbiotic functions. *Microbial Cell Factories* **5**: 7.

Smit P, Limpens E, Geurts R, Fedorova E, Dolgikh E, Gough C, Bisseling T. 2007. Medicago LYK3, an entry receptor in rhizobial nodulation factor signaling. *Plant Physiology* **145**: 183–191.

Sugawara M, Takahashi S, Umehara Y, Iwano H, Tsurumaru H, Odake H, Suzuki Y, Kondo H, Konno Y, Yamakawa T *et al.* 2018. Variation in bradyrhizobial NopP effector determines symbiotic incompatibility with Rj2-soybeans via effector-triggered immunity. *Nature Communications* **9**: 3139.

Sugawara M, Umehara Y, Kaga A, Hayashi M, Ishimoto M, Sato S, Mitsui H, Minamisawa K. 2019. Symbiotic incompatibility between soybean and Bradyrhizobium arises from one amino acid determinant in soybean Rj2 protein. *PLoS ONE* **14**: e0222469.

Tang F, Yang S, Liu J, Zhu H. 2016. Rj4, a gene controlling nodulation specificity in soybeans, encodes a thaumatin-like protein but not the one previously reported. *Plant Physiology* **170**: 26–32.

Toruño TY, Shen M, Coaker G, Mackey D. 2018. Regulated disorder: posttranslational modifications control the RIN4 plant immune signaling hub. *Molecular Plant Microbe Interactions* **32**: 56–64.

Tóth K, Kim D, Cho S-H, Nguyen CT, Nguyen THN, Hartanto C, Michno J-M, Stec AO, Stupar RM, Stacey G. 2023. Soybean RIN4 represents a mechanistic link between plant immune and symbiotic signaling. *eLife* **12**: RP93149.

Wang D, Jin R, Shi X, Guo H, Tan X, Zhao A, Lian X, Dai H, Li S, Xin K *et al.* 2025. A kinase mediator of rhizobial symbiosis and immunity in Medicago. *Nature* **643**: 768–775.

Wang Y, Tang H, DeBarry JD, Tan X, Li J, Wang X, Lee T, Jin H, Marler B, Guo H *et al.* 2012. MCScanX: a toolkit for detection and evolutionary analysis of gene synteny and collinearity. *Nucleic Acids Research* **40**: e49.

Wilton M, Subramaniam R, Elmore J, Felsensteiner C, Coaker G, Desveaux D. 2010. The type III effector HopF2 Pto targets Arabidopsis RIN4 protein to promote *Pseudomonas syringae* virulence. *Proceedings of the National Academy of Sciences, USA* **107**: 2349–2354.

Yang S, Tang F, Gao M, Krishnan HB, Zhu H. 2010. R gene-controlled host specificity in the legume–rhizobia symbiosis. *Proceedings of the National Academy of Sciences, USA* **107**: 18735–18740.

Yano K, Aoki S, Liu M, Umehara Y, Suganuma N, Iwasaki W, Sato S, Soyano T, Kouchi H, Kawaguchi M. 2017. Function and evolution of a *Lotus japonicus* AP2/ERF family transcription factor that is required for development of infection threads. *DNA Research* **24**: 193–203.

Zhang B, Wang M, Sun Y, Zhao P, Liu C, Qing K, Hu X, Zhong Z, Cheng J, Wang H *et al.* 2021. Glycine max NNL1 restricts symbiotic compatibility with widely distributed bradyrhizobia via root hair infection. *Nature Plants* 7: 73–86.

Supporting Information

Additional Supporting Information may be found online in the Supporting Information section at the end of the article.

Fig. S1 Sequential and structural alignment of LjCyPAs and AtROC1.

Fig. S2 mRNA abundance of *LjCyPA1*, *LjCyPA2*, and *LjCyPA3* in early-infection stage.

Fig. S3 Schematic illustration of CRISPR/Cas9-induced nonsense mutation in *LjCyPAs*.

Fig. S4 Number of infection threads in MG-20 wild-type and *cypA1* another mutant allele (*LjcypA1-2*).

Fig. S5 Infection thread numbers in *LjcypA1-1* mutant are restored in hairy roots expressing *LjCyPA1*.

Fig. S6 High-resolution images of abnormal infection threads at the elongation stages in *LjcypA1-1* mutant.

Fig. S7 Transcriptomic differences in response to inoculation with *M. loti* ΔT3SS mutant in MG-20 and *LjcypA1-1* mutant.

Fig. S8 Quantitative RT-PCR analysis of immune-/defense-related and symbiotic gene expression in MG-20 and *LjcypA1-1* mutant, with or without *M. loti* MAFF303099 or its ΔT3SS mutant.

Fig. S9 Gain-of-function of *LjCyPA1* promotes symbiosis with *M. loti* MAFF303099 and the *M. loti* ΔT3SS.

Fig. S10 Bimolecular fluorescence complementation between LjCyPA1 and LjRIN4.

Fig. S11 *CyPA2* and *CyPA3* conservation in representative legumes and nonlegumes.

Table S1 Gene IDs and names of the T3SS cluster deleted in this study for mutant construction.

Table S2 List of primers.

Table S3 Differential gene expression in RNA-seq.

Please note: Wiley is not responsible for the content or functionality of any Supporting Information supplied by the authors. Any queries (other than missing material) should be directed to the *New Phytologist* Central Office.